ELSEVIER

CrossMark

Alzheimer's & Dementia: Translational Research & Clinical Interventions 3 (2017) 92-106

Alzheimer's & Dementia

Featured Article

Combination treatment with leptin and pioglitazone in a mouse model of Alzheimer's disease

Carmen M. Fernandez-Martos*, Rachel A. K. Atkinson, Meng I. Chuah, Anna E. King, James C. Vickers

Wicking Dementia Research and Education Centre, Faculty of Health, University of Tasmania, Hobart, Tasmania, Australia

Abstract

Introduction: Combination therapy approaches may be necessary to address the many facets of pathologic change in the brain in Alzheimer's disease (AD). The drugs leptin and pioglitazone have previously been shown individually to have neuroprotective and anti-inflammatory actions, respectively, in animal models.

Methods: We studied the impact of combined leptin and pioglitazone treatment in 6-month-old APP/PS1 (APPswe/PSEN1dE9) transgenic AD mouse model.

Results: We report that an acute 2-week treatment with combined leptin and pioglitazone resulted in a reduction of spatial memory deficits (Y maze) and brain β-amyloid levels (soluble β-amyloid and amyloid plaque burden) relative to vehicle-treated animals. Combination treatment was also associated with amelioration in plaque-associated neuritic pathology and synapse loss, and also a significantly reduced neocortical glial response.

Discussion: Combination therapy with leptin and pioglitazone ameliorates pathologic changes in APP/PS1 mice and may represent a potential treatment approach for AD.

Keywords: Alzheimer's disease (AD); Treatment; Leptin; Pioglitazone

1. Introduction

Alzheimer's disease (AD), the most common form of dementia, is an aging-related complex neurodegenerative disease that leads to progressive impairment in cognitive function [1,2]. No current therapeutic disease-modifying intervention exists for human AD, although a range of monotherapies (including anti–amyloid-β (Aβ) peptide antibodies, secretase inhibitors, and anti-inflammatory agents, e.g., pioglitazone) have demonstrated efficacy in different transgenic (Tg) mice models of AD. Indeed, these therapeutic agents have a potential to be used as combination therapy; however, only a few studies have used this approach. For example, Chow et al. [3] demonstrated that the genetic reduction of both γ-secretase and β-secretase 1 (BACE1) additively attenuates the Aβ levels and ameliorates cognitive deficits occurring in aged APP/PS1 mice. Jacobsen et al. [4] determined that combined treatment with the anti-Aβ antibody gantenerumab and the BACE1 inhibitor RO5508887 enhanced Aβ reduction in APP_{London} mice. In addition, combined liver X receptor agonist GW3965 and the PPARγ agonist pioglitazone reduced Aβ plaques, produced anti-inflammatory effects, and mediated behavioral improvements in APP/PS1 mice [5]. Hence, given the likely range of cellular and pathologic changes associated with AD, combination therapies targeted at more than one aspect of the spectrum of disease-related degenerative pathways may be a useful approach. In this regard, we have now examined a combination of a putative neuroprotective hormone (leptin, L) with an agent which regulates the inflammatory response (pioglitazone, P).

Leptin is a polypeptide hormone, primarily secreted by adipocytes, that exerts its main biological function in the brain

*Corresponding author. Tel.: +61 3 62264673; Fax: +61 3 6226 4880.
E-mail address: Carmen.fernandezmartos@utas.edu.au

http://dx.doi.org/10.1016/j.trci.2016.11.002

[6,7]. Recent studies conducted in several Tg animal AD models have demonstrated the potential neuroprotective beneficial effects of leptin resulting in reduction of Aβ levels [8–12] and intracellular tau phosphorylation in vitro [13,14] and in vivo [8]. In addition, leptin has been shown to improve memory processing and modulates long-term potentiation and synaptic plasticity in rodent experimental models [15–17], which suggests a potential role of leptin in preventing cognitive decline.

Pioglitazone, a member of the class of the thiazolidinediones (TZDs), has proven effective in several Tg models of AD, mainly resulting in reduction of inflammatory cytokines [18,19], oxidative stress [20], and glial activation [19,20]. Importantly, clinical studies have shown that TZDs re-establish glucose regulation and normal lipid levels, reduce inflammation and Aβ peptide, and increase cerebral blood flow [21–23].

Our study evaluated the impact of a combination of leptin and pioglitazone (L + P) on brain pathology and cognitive function in the APP/PS1 (APPswe/PSEN1dE9) Tg line. The treatment was administered acutely for 2 weeks to 6-month-old APP/PS1 mice because it has been shown that 7 days of treatment with pioglitazone can act rapidly to inhibit inflammatory responses in the brain and negatively modulate amyloidogenesis [19]. In addition, acute leptin administration has been demonstrated to be neuroprotective under degenerative conditions [24]. Importantly, in the APP/PS1 mice, brain Aβ deposits appear at 4 months of age and increase up to 6 months of age [25]. Severe gliosis starting around 6 months, especially in the vicinity of plaques, is paralleled with increasing plaque deposition [26]. These neuropathologic characteristics allowed us to examine whether the acute neuroprotective actions of L + P therapy given at 6 months of age have beneficial downstream effects at 8 months of age, in the background of increasing brain Aβ levels and gliosis. This study shows that L + P therapy significantly (1) reduced cerebral Aβ levels and hippocampus-dependent spatial memory deficits, (2) reduced neocortical neurite susceptibility, (3) alleviated synaptic alterations, and (4) reduced the glial response, altering the expression of genes involved in inflammation and oxidative stress. These results support that the neuroprotective effect of leptin in combination with the anti-inflammatory action of pioglitazone significantly attenuates pathologic features which characterize AD.

2. Methods

2.1. Experimental design and drug treatments

Cohorts of male APP/PS1 mice [27] and age-matched wild-type (WT) littermates were used in this study. The WT and APP/PS1 mice (n = 20/genotype) were divided into four subgroups (n = 10/subgroup), and one subgroup from each genotype received the combination drug treatment of 0.03 mg/kg/d intranasal (IN) recombinant mouse leptin (Sigma-Aldrich) [28] together with the intraperitoneal injection of 10 mg/kg/d of pioglitazone [29] (1:3 dimethyl sulfoxide [DMSO]:phosphate-buffered saline [PBS], pH 7.2; Cayman Chemical) daily for 2 consecutive weeks. Recombinant mouse leptin was prepared in 0.125% (2.3 mM) of *N*-tetradecyl-b-D-maltoside (TDM) (Sigma-Aldrich) reconstituted in PBS (pH 7.2) at a concentration of 1 mg/mL. The alkylglycoside, TDM, was used to increase the bioavailability of leptin for IN administration [30]. IN administration was conducted as previously described [31,32]. Briefly, a 1-mL tuberculin syringe fitted with a no.27 needle bearing a plastic tube at the end was used to deliver 20 μL of leptin-TDM or vehicle (VH; PBS-TDM) into the nasal cavity via one of the external nares, unilaterally under brief superficial isoflurane anesthesia (3% isoflurane in 100% oxygen). Mice were monitored closely in terms of their mobility or level of activity immediately after the procedure. Pioglitazone was administrated immediately after the IN drug delivery. Control groups of each genotype received the combination IN and intraperitoneal VH solutions (PBS-TDM and 1:3 DMSO:PBS; pH 7.2) daily for 2 consecutive weeks. No difference in body weight gain between treatment groups was observed (Supplementary Fig. 1). The maintenance and use of mice and all experimental procedures were approved by the Animal Ethics Committee of the University of Tasmania (A13939), in accordance with the Australian Guidelines for the Care and Use of Animals for Scientific Purposes. All analyses were conducted by personnel blinded to the animal genotype.

2.2. Y maze test

Spatial short-term recognition memory (novel arm discrimination) was assessed using the Y maze [33]. The Y maze test was assessed in WT and APP/PS1 mice (n = 20/genotype) at 5.5 months of age to determine cognitive differences between genotypes before drug administration at 6 months of age. Mice were retested at 7.5 months before sample processing at 8 months of age. Animals were habituated to the test room and to human handling 5 days before the Y maze test. Briefly, the Y maze consists of three arms placed 120° apart, with a black and white visual cue at the end of each arm. All mice underwent an initial training trial, in which a randomly assigned arm of the Y maze was blocked (novel arm). Mice were randomly designated to and placed in a start arm facing the wall of the arm and were allowed to explore the two open arms for 10 minutes. After a training trial, mice were returned to their home cage for the 1-hour intertrial interval. The testing phase began 1 hour after the training phase. Mice were entered into the designated start arm as in training and were able to freely explore all arms of the maze including the novel arm. Mice were allowed to explore the Y maze for 5 minutes after leaving the start arm. Y maze testing was recorded where percentage (%) of time spent in the novel arm was analyzed by a video tracking system and analysis software (EthoVision XT; Noldus).

2.3. Tissue preparation

Animals were terminally anesthetized with sodium pentobarbitone (140 mg/kg) and transcardially perfused with 0.01 M PBS (pH 7.4) or 4% paraformaldehyde. Brains were immediately dissected, postfixed overnight in the same fixative solution, and then transferred to 18% and then 30% sucrose solutions overnight [34]. Serial coronal cryosections (40 μm thick) were cut on a cryostat (Leica CM 1850). For molecular biology experiments, the neocortex and hippocampus for each animal were split into two fractions and processed independently, for real-time polymerase chain reaction (PCR) or Western blot analysis. Cortex and hippocampal samples were stored at −80°C for later analysis.

2.4. RNA isolation and RT-qPCR

Total RNA was isolated from neocortical and hippocampal samples, respectively, using the RNeasy Mini Kit (Qiagen), according to the manufacturer's instructions. Complementary DNA (cDNA) was synthesized as described previously [35]. Relative quantitation of *APP* was performed using 10 ng of reverse-transcribed total RNA (cDNA) in TaqMan One-Step real-time PCR Master Mix (PE Applied Biosystem) and using a Pre-Developed TaqMan Assay (Mm01344172_m1) (PE Applied Biosystem). This predeveloped APP TaqMan assay can detect a region of homology between both human and mouse versions of *APP* gene [36]. β-Actin (Mm00607939_s1) with VIC as real-time reporter was used as a control to normalize gene expression. Furthermore, relative quantitation of *IL-1*β*, IL-6, TNF-*α*,* and *iNOS* was performed using 25 ng of reverse-transcribed total RNA, 20 pmol/mL of both sense and antisense primers, and the SYBR Green PCR Master Mix (Applied Biosystems) in a final reaction volume of 10 μL [37]. The reactions were run on a LightCycler 480 system instrument and software (Roche). Relative quantification for each gene was performed by the ΔΔCt method [38]. Primers were designed using NCBI/Primer-BLAST software (Table 1), and β-actin (primer sequence obtained from [39]) was used as an endogenous control.

2.5. Protein extraction and Western blot analysis

Proteins from neocortical and hippocampal tissues were extracted with RIPA buffer (Sigma-Aldrich) containing a cocktail of protease inhibitors (Roche). Denatured protein samples (20 μg) from each group were electrophoresed into Bolt Bis-Tris Plus gels (Invitrogen, Camarillo, CA, USA), transferred to PVDF membranes (BioRad) and incubated with primary antibodies (rabbit anti-synaptophysin [SYN, 1:1000; Millipore], mouse anti-PSD-95 [1:1000; Abcam], rabbit anti-vGLUT1 [1:1000; Synaptic Systems], mouse anti-GAD65 [1:1000; Abcam] and mouse anti-GAD67 [1:1000; Millipore], anti-GFAP [1:1000; Dako], and anti-Iba1 [1:1000; Synaptic Systems]) overnight. Subsequently, a corresponding antirabbit or antimouse horseradish peroxidase–conjugated secondary antibody (1:7000; Dako) was used, as described previously [40]. β-Actin (1:7000, Sigma) was used as a loading control, and band intensity was measured as the integrated intensity using ImageJ software (v1.4; NIH).

2.6. Measurement of Aβ ($Aβ_{1–42}$) peptide in neocortical and hippocampal tissues by ELISA

Soluble human $Aβ_{1–42}$ was measured in neocortical and hippocampal extracts by an enzyme-linked immunosorbent assay (ELISA) kit (Invitrogen). Tissues were processed as outlined in Section 2.5. Soluble human $Aβ_{1–42}$ levels were normalized to total protein levels, and neocortical and hippocampal homogenates were expressed as picograms of $Aβ_{1–42}$ content per milligrams of total proteins (pg/mg). Values were determined using a four-parameter nonlinear regression equation.

2.7. Immunofluorescence and thioflavin-S staining

All immunohistochemical procedures were performed as previously described [41] in APP/PS1 L + P mice (n = 5/genotype) and VH (n = 5/genotype) mice tissues, respectively. Mouse coronal sections (40 μm thick) were labeled for mouse anti-Pan-Axonal Neurofilament Marker (SMI 312) (1:1000; Covance), mouse anti-MOAβ-2 (1:1000; Novus Biologicals), rabbit anti-GFAP (1:500; Dako), and rabbit anti-Iba1 (1:500; Wako). Tissue was stained with thioflavin-S (Sigma-Aldrich) as previously described [42]. Immunolabeling of Aβ plaques using the MOAβ-2 antibody was conducted after formic acid treatment of sections [43]. Primary antibody binding was visualized using species-specific fluorescent secondary antibodies conjugated to Alexa Fluor 488 and 594 (1:500; Invitrogen), respectively,

Table 1
List of qRT-PCR primers

Gene name	Forward primer	Reverse primer	Acc no.
IL1-β	5′-GCTTCAGGCAGGCAGTATCA-3′	5′-AAGGTCCACGGGAAAGACAC-3′	NM_008361.3
IL-6	5′-CCAGTTGCCTTCTTGGGACT-3′	5′-GTGAAGTAGGGAAGGCCGTG-3′	NM_031168.1
TNF-α	5′-AGCCGATGGGTTGTACCTTG-3′	5′-ATAGCAAATCGGCTGACGGT-3′	NM_013693.3
iNOS	5′-CTCGGAACTGTAGCACAGCA-3′	5′-GTTGCCATTGTTGGTGGCAT-3′	NM_010927.3

NOTE. Primers used for qRT-PCR analysis of the genes assessed, including the gene symbol, primer sequence (forward and reverse sequence respectively) and GenBank accession number. The primers used to assess the expression of the internal control β-actin not included in the list were obtained elsewhere [39].

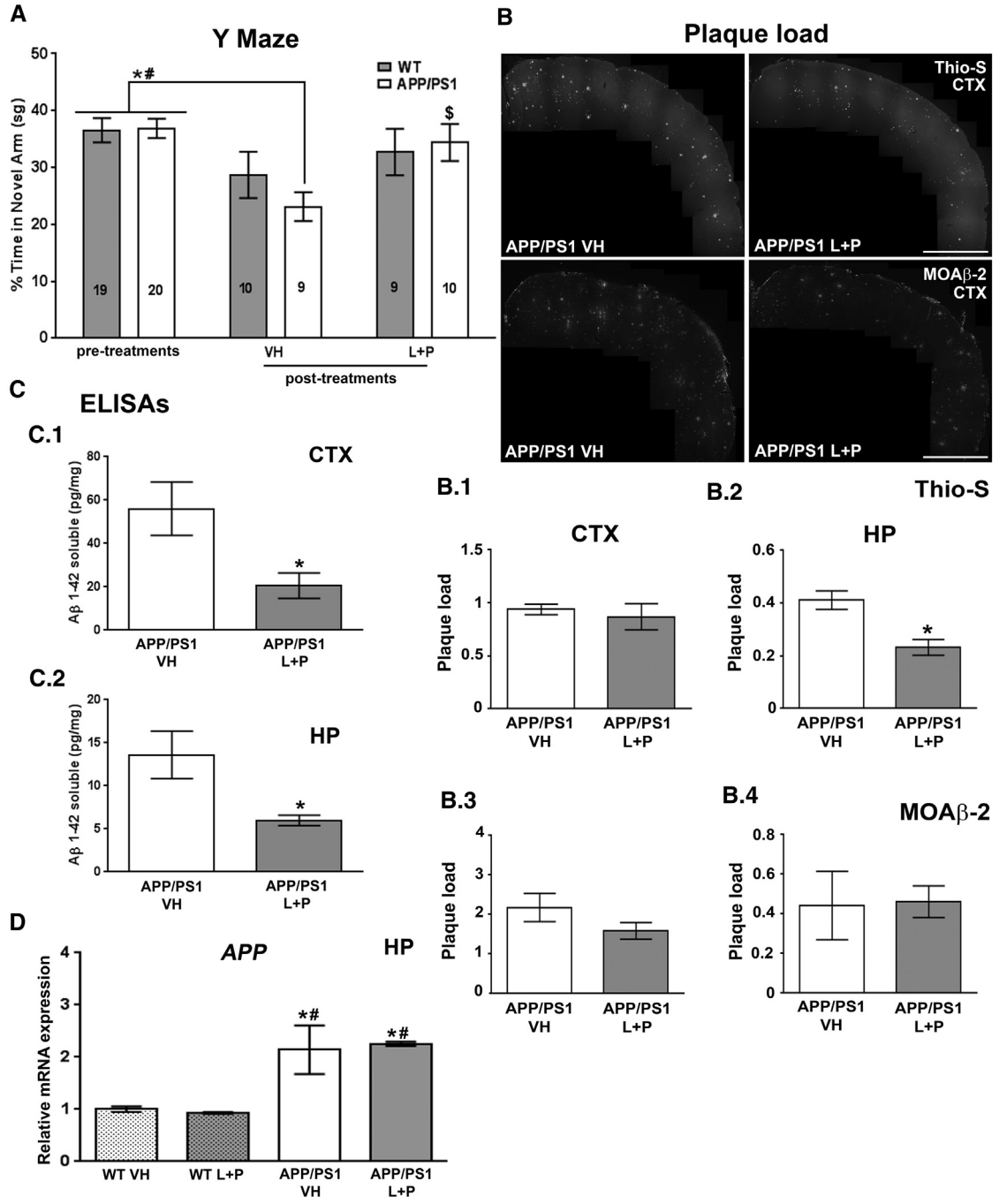

Fig. 1. Leptin and pioglitazone treatment reduced cerebral Aβ levels and memory loss. (A) The results of the Y maze demonstrating no differences on short-spatial memory function before drug administration (pre-treatment) at 5.5-month-old mice between APP/PS1 and WT mice. However, there was a significant spatial memory function loss at 7.5-month-old mice in APP/PS1 VH mice compared with pretreatment values ($^{*}P < .01$). The acute treatment with L + P had a significant impact on spatial memory loss in APP/PS1 mice ($^{\$}P < .05$, post hoc Sidak's multiple comparison test). (B) An example of images of Aβ plaque immunoreactivity in the neocortex of an APP/PS1 mouse after VH and L + P treatments. Plaque load analysis showed no differences in thioflavin-S–positive deposits in the neocortex in APP/PS1 L + P mice compared with APP/PS1 VH mice (B.1), whereas L + P treatment significantly decreased thioflavin-S–positive deposits in hippocampus in APP/PS1 mice (B.2) ($^{*}P < .01$, Student *t* test). In addition, L + P treatment induced a modest decrease in neocortical Aβ deposition in APP/PS1 mice (B.3), whereas no difference was detected in the hippocampus in APP/PS1 L + P mice compared with APP/PS1 VH mice (B.4). (C) ELISA analysis demonstrated that L + P combination significantly decreased neocortical ($^{*}P < .05$, Student *t* test) and hippocampal ($^{*}P < .05$, Student *t* test) soluble $A\beta_{1-42}$ levels in APP/PS1 mice. (D) Hippocampal mRNA expression of the *APP* transcript was assessed by qRT-PCR using a TaqMan probe recognizing both mouse and human forms of *APP* gene, and although we detected approximately a two to threefold increase in *APP* transcript in the hippocampus of APP/PS1 mice compared with both WT VH mice ($^{*}P < .01$) and WT L + P mice ($^{\#}P < .05$ post hoc Sidak's multiple comparison test), L + P combination did not alter *APP* transcripts in APP/PS1 mice. Bar graphs represent the mean ± standard error of the mean. Statistical analyses were performed by two-way analysis of variance followed by Dunnett test, unless stated otherwise. Abbreviations: CTX, neocortex; HP, hippocampus. Scale bar = 500 μm.

and slides coverslipped with Immu-Mount mounting medium (Thermo Scientific). In all cases, the specificity of immunoreactivity was confirmed by processing sections lacking primary antibody.

2.8. Analysis of Aβ deposition

Quantitation of brain Aβ deposition (thioflavin-S or MOAβ-2 immunolabeling) in the neocortex and hippocampus was performed for both APP/PS1 L + P and APP/PS1 VH mice, as previously described [41]. Briefly, five serial coronal sections evenly spaced across the rostrocaudal axis of the brain (from bregma 1.42 mm to −2.54 mm, 800 μm apart), according to the stereotaxic mouse atlas of Franklin and Paxinos [44], were labeled with the MOAβ-2 antibody (anti-Aβ antibody). In addition, five coronal sections were stained with thioflavin-S, which detects fibrillar Aβ deposits. All staining and immunohistochemistry were performed at the same time to reduce batch-to-batch variation. Images were acquired (×10 objective, Leica DM LB2 microscope, NIS-Elements D Imaging Software, Nikon Instruments, USA) of the entire hippocampal formation when present, and one hemisphere of the neocortex dorsal to the rhinal fissure of each tissue section. Images were manually outlined and automatically thresholded (NIH ImageJ, version 1.45p) according to the stained signal, which was maintained for all images. The % area stained by thioflavin-S and labeled with MOAβ-2 in the neocortex and hippocampus was then calculated by dividing the total labeled area by the total area analyzed. All analyses were conducted by personnel blinded to animal genotype.

2.9. Analysis of dystrophic neurites

Quantitation of neocortical dystrophic neurites (DNs) (in thioflavin-S–stained sections co-labeled for neurofilament

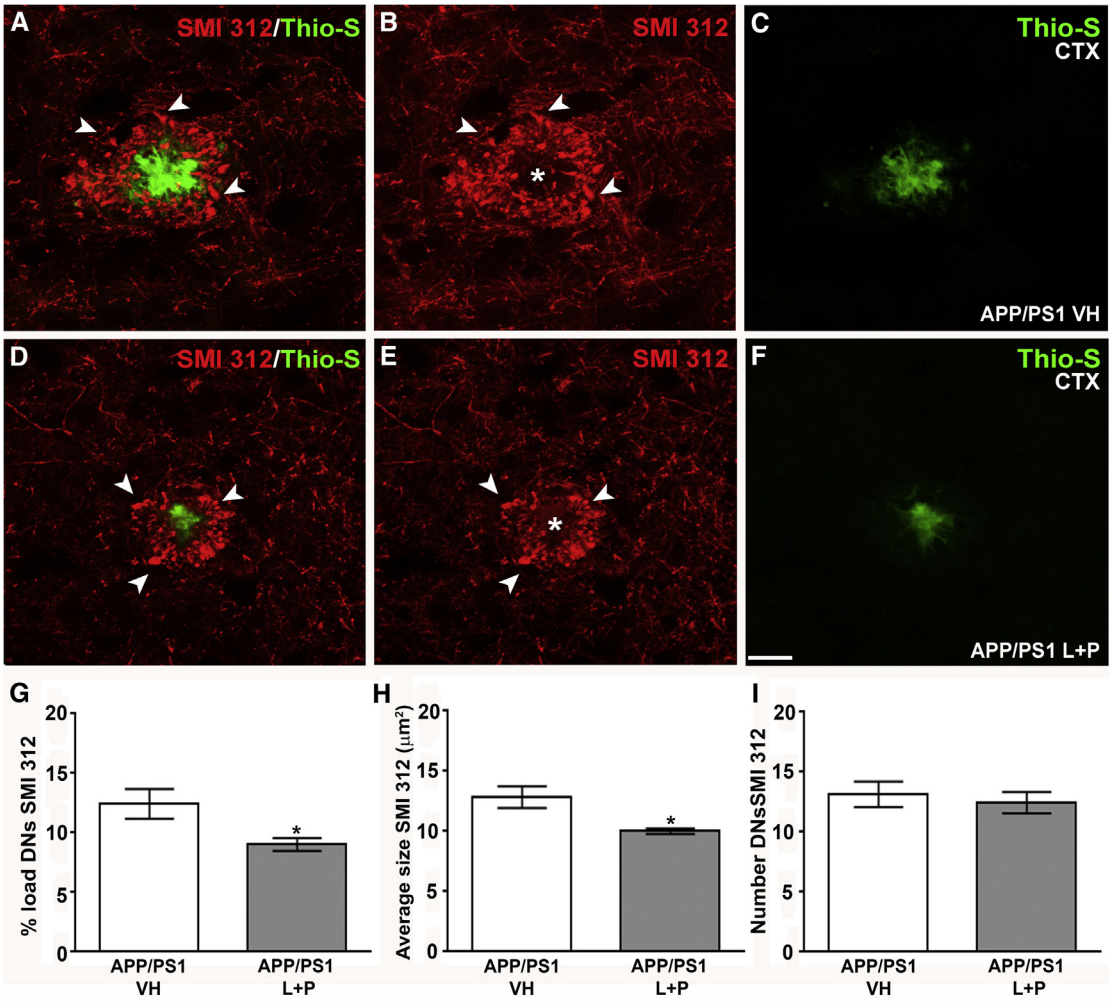

Fig. 2. Leptin and pioglitazone treatment reduces neocortical NF-containing DNs. (A–C) Representative images of SMI 312–labeled DNs surrounding thioflavin-S plaques (represented by asterisk) are shown for APP/PS1 VH mice and APP/PS1 L + P (D–F) mice. The percentage area occupied by SMI 312–labeled DNs (G) (*$P < .05$) and the average DNs size (H) (*$P < .05$) were decreased in APP/PS1 L + P mice compared to APP/PS1 VH mice. There was no difference in the average number of DNs between genotypes (I). Bar graphs represent the mean ± standard error of the mean. *P* values (unpaired comparisons) by two-tailed Student's *t* test, unless stated otherwise. Scale bars = 20 μm. Arrowheads indicate DNs. Abbreviation: CTX, neocortex.

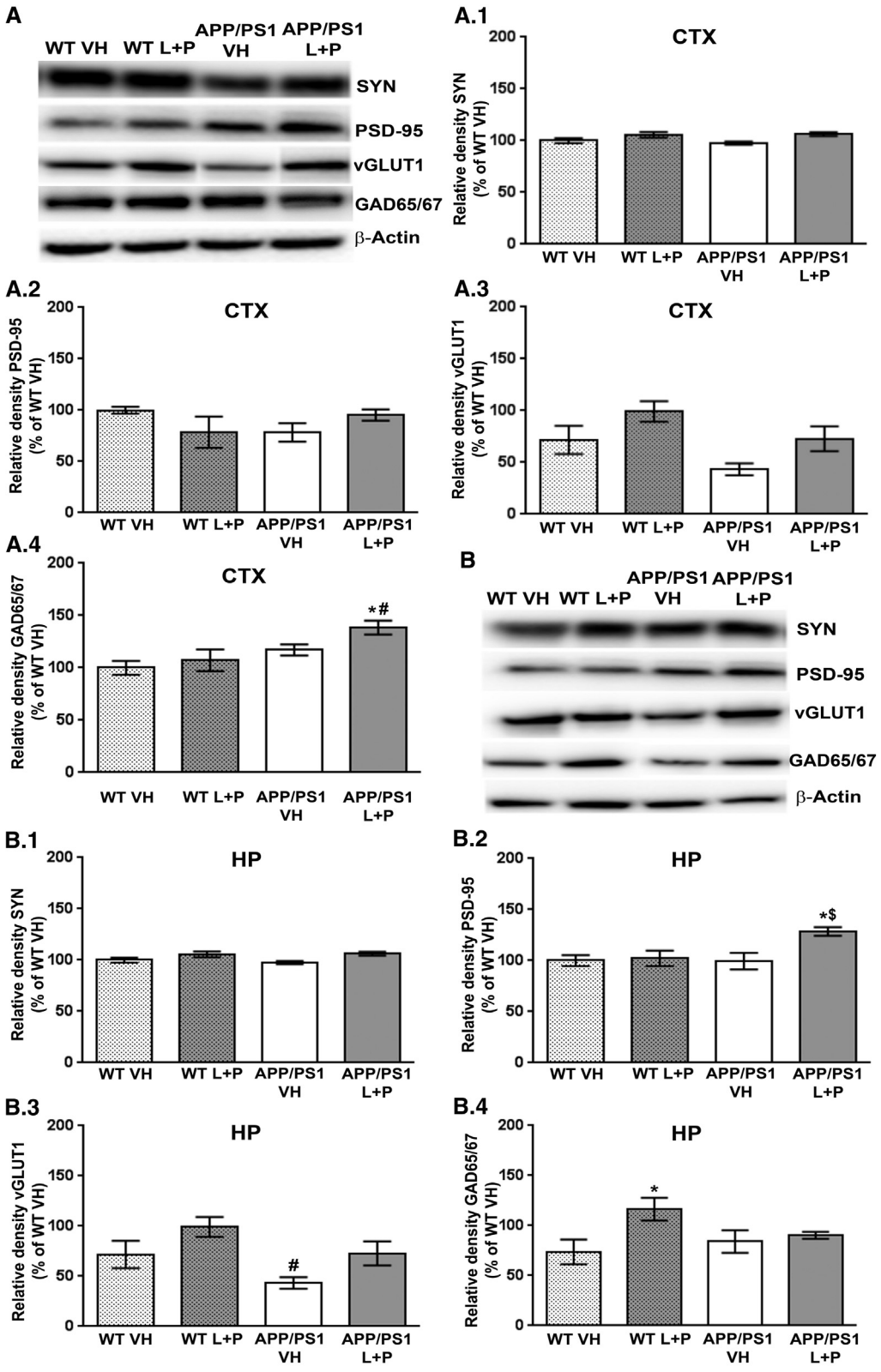

Fig. 3. Effect of leptin and pioglitazone treatment on synaptic protein levels. (A and B) Representative β-actin–normalized immunoblot images and quantitation of SYN (A.1 and B.1), PSD-95 (A.2 and B.2), vGLUT1 (A.3 and B.3), and GAD65/67 (A.4 and B.4) synaptic proteins in neocortical/hippocampal extracts of WT VH mice, WT L + P mice, APP/PS1 VH mice, and APP/PS1 L + P mice. L + P therapy did not produce significant differences in synaptophysin levels in neocortex/hippocampus homogenates across groups analyzed. There were no significant differences in neocortical PSD-95 levels across groups analyzed; however, a significant hippocampal upregulation of PSD-95 protein was observed in APP/PS1 L + P mice relative to WT VH mice ($*P < .05$) and compared to APP/PS1 VH mice ($^{\$}P < .05$ post hoc Sidak's multiple comparison test). In both neocortex/hippocampus homogenates, a modest increase in vGLUT1 levels was

markers) was performed in 10 coronal sections (40 μm; bregma position −2.54 mm) from both APP/PS1 L + P and APP/PS1 VH mice, respectively as previously described [41]. Briefly, images of plaques were acquired across the retrosplenial dysgranular cortex, somatosensory cortex, auditory cortex, and entorhinal cortex dorsal to the rhinal fissure according to the stereotaxic mouse atlas of Franklin and Paxinos [44]. To classify neurites as dystrophic, we used previously described criteria for synaptic and cytoskeletal pathology in abnormal neuronal processes associated with plaques [45–48]. Confocal z-stack images (1 μm/z-stack) were collected using the same acquisition parameters on a spinning disk UltraVIEW VoX 3D Live Cell Imaging System confocal microscope, with ×40 objective and Volocity Imaging software (Perkin Elmer, USA). A donut-shaped region of interest with a 20 μm radius was centered over the plaque, the DNs within this region of interest were then thresholded (NIH ImageJ version 1.45p) according to the immunohistochemical signal, and this threshold level was maintained for all images. Particles $<2.0\ \mu m^2$ were not quantified. Using these parameters, we determined the number, average size, and percentage area occupied by SMI 312–labeled DNs. Analysis was conducted by personnel blinded to the animal treatments.

2.10. Statistical analysis

The nonparametric Student *t* test was used in the analysis of Aβ deposition, ELISAs, DNs, and Y maze, respectively, for comparisons between APP/PS1 L + P and APP/PS1 VH mice. In the analysis of Y Maze, real-time PCR and Western blot two-way analysis of variance was used followed by Dunnett's post hoc test, to compare all groups with control WT VH mice, while Sidak's post hoc test was used for multiple comparisons between all groups. Changes in body weight were analyzed by repeated measures followed by Bonferroni post hoc test. Statistical analysis was performed using GraphPad Prism software (version 6.0) with $P < .05$ (95% CI) considered significant. Values are reported as means ± standard error of the mean.

3. Results

3.1. The combination treatment of leptin and pioglitazone reduced cerebral Aβ levels and attenuated memory deficits

We tested cognitive performance in APP/PS1 and WT mice before L + P administration (5.5 months of age; Fig. 1A), and there was no effect of genotype in Y maze performance at this age. At 7.5 months of age, Dunnett's post hoc test demonstrated a significant reduction of spatial short-term recognition memory performance in APP/PS1 VH mice compared with pretreatment basal performance. However, Sidak's post hoc test demonstrated that L + P therapy significantly attenuated this spatial memory performance deficit in APP/PS1 mice at this age (Fig. 1A). Student *t* test revealed no significant differences in the percentage of neocortical area occupied by fibrillar Aβ deposits in APP/PS1 mice treated with L + P therapy relative to VH mice (Fig. 1B.1–4), while L + P treatment resulted in a statistically significant decrease in the percentage of hippocampal area occupied by fibrillar Aβ plaques as compared to APP/PS1 VH mice (Fig. 1B.1 and 2). Notably, Student *t* test demonstrated that L + P therapy did not result in differences in MOAβ-2–labeled Aβ load in either neocortex or hippocampus in APP/PS1 mice relative to VH mice (Fig. 1B.3 and 4). Student *t* test demonstrated that soluble $A\beta_{1-42}$ peptide was significantly decreased in both neocortical and hippocampal homogenates of APP/PS1 mice treated with L + P relative to VH (Fig. 1C.1 and 2). Finally, there was a significant effect of genotype in the hippocampal APP mRNA levels. Indeed, we detected approximately a twofold to threefold increase in *APP* transcript in the hippocampus of APP/PS1 mice compared with both WT VH controls and WT L + P mice (Fig. 1D), which was not unexpected given that the human mutated *APP* gene is overexpressed in this model. However, Sidak's post hoc test demonstrated that L + P combination did not alter *APP* expression in APP/PS1 mice (Fig. 1D).

3.2. The combination treatment with leptin and pioglitazone was associated with reduced DN pathology

Abundant neurofilament-labeled DNs surrounding thioflavin-S plaques were localized to the neocortex of APP/PS1 L + P and APP/PS1 VH mice (Fig. 2A–F). Student *t* test demonstrated that L + P therapy significantly reduced the percentage area occupied by SMI 312–labeled DNs associated with plaques in APP/PS1 mice (Fig. 2G), which was associated with a significant decrease in the average size of the SMI 312–labeled DNs (Fig. 2H). In contrast, Student *t* test demonstrated that there was no significant difference in the number of SMI 312–labeled DNs in APP/PS1 L + P compared with APP/PS1 VH mice (Fig. 2I).

3.3. The combination treatment with leptin and pioglitazone affected synaptic protein expression

Immunoblotting analysis demonstrated that there was no effect of genotype and treatments in the expression of the

detected in APP/PS1 mice treated with L + P, while only a statistically significant upregulation of vGLUT1 was observed in the hippocampus of APP/PS1 VH compared with WT L + P mice ($^{\#}P < .05$ post hoc Sidak's multiple comparison test). Finally, L + P therapy significantly increased neocortical GAD65/67 levels in APP/PS1 mice relative to WT VH mice ($^{*}P < .01$) and WT L + P mice ($^{\#}P < .05$ post hoc Sidak's multiple comparison test). In addition, L + P therapy significantly increased hippocampal GAD65/67 levels in WT mice relative to WT VH controls ($^{*}P < .05$). The data are presented as a percentage (%) of the corresponding value in the WT VH control group. Bar graphs represent the mean ± standard error of the mean. Statistical analyses were performed by two-way analysis of variance followed by Dunnett test, unless stated otherwise. Abbreviations: CTX, neocortex; HP, hippocampus.

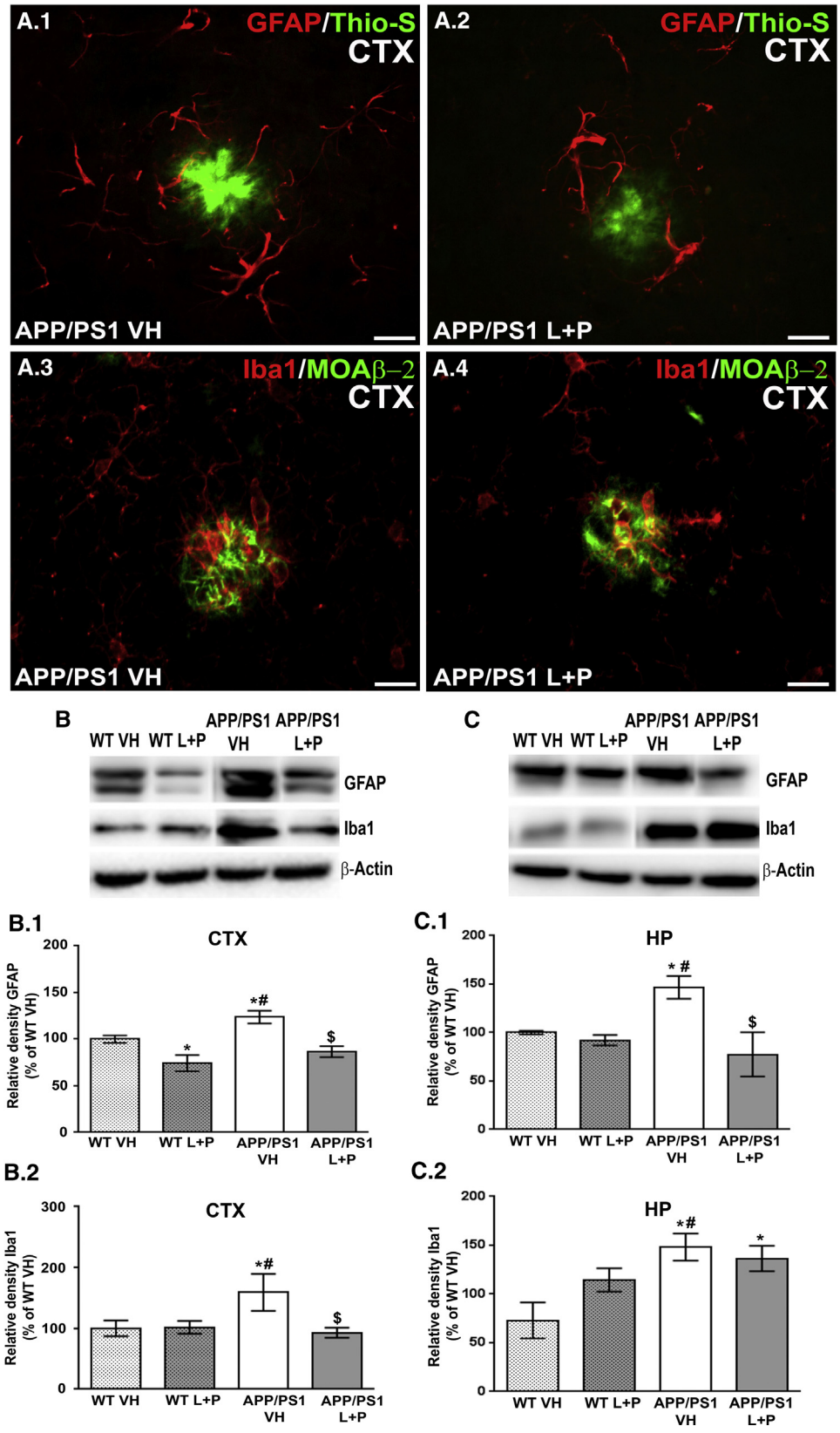

Fig. 4. Effect of leptin and pioglitazone treatment on brain glial response. Representative images of both GFAP+ astrocytes (A.1 and A.2) and Iba1+ microglia (A.3 and A.4) surrounding Aβ plaques in APP/PS1 VH mice and APP/PS1 L + P mice. (B and C) Representative β-actin–normalized immunoblot images and quantitation of GFAP and Iba1 proteins in neocortical (B.1 and 2) and hippocampal (C.1 and 2) extracts of WT VH mice, WT L + P mice, APP/PS1 VH mice, and APP/PS1 L + P mice. In the neocortex, GFAP expression was significantly higher in APP/PS1 mice relative to WT VH mice (*$P < .01$) and compared to WT

pan-presynaptic marker SYN in neocortex/hippocampus homogenates across groups (Fig. 3A.1 and B.1). However, Sidak's post hoc test demonstrated that a statistically significant hippocampal upregulation of PSD-95 levels relative to APP/PS1 VH mice was observed using L + P therapy (Fig. 3B.2). Finally, Sidak's post hoc test demonstrated a significant increase in GAD65/67 levels in APP/PS1 L + P mice relative to VH and WT L + P mice in the neocortex (Fig. 3A.4), but not in the hippocampus (Fig. 3B.4).

3.4. The combination treatment with leptin and pioglitazone reduced the glia response to Aβ pathology and influenced the expression of genes linked to inflammation and oxidative stress

Activated astrocytes and microglia were present in the brain of both APP/PS1 VH and APP/PS1 L + P mice surrounding Aβ plaques (Fig. 4A). Dunnett's post hoc test demonstrated that L + P therapy significantly decreased both neocortical and hippocampal GFAP levels in APP/PS1 mice (Fig. 4B.1 and C.1), while in WT treated mice relative to WT VH, a statistically significant reduction of GFAP was observed only in the neocortex (Fig. 4B.1). As expected, Dunnett's post hoc test demonstrated that Iba1 expression was significantly higher in neocortex/hippocampus homogenates in APP/PS1 VH mice relative to WT VH controls (Fig. 4B.2 and C.2). Interestingly, Sidak's post hoc test demonstrated that L + P therapy significantly decreased neocortical Iba1 levels in APP/PS1 mice (Fig. 4B.2), but not in the hippocampus (Fig. 4C.2), while it also did not affect the expression levels in WT treated mice relative to WT VH controls.

Real-time PCR (RT-qPCR) analysis demonstrated that L + P treatment, relative to VH, was associated with a significant decrease in *IL-1β, IL-6, TNF-α,* and *iNOS* transcripts in the neocortex of APP/PS1 mice (Fig. 5A.1–4). In contrast, a different profile of expression was present in hippocampus (Fig. 5B.1–4). Accordingly, Sidak's post hoc test demonstrated a significant downregulation of IL-6 mRNA in APP/PS1 L + P mice compared with APP/PS1 VH mice, and no statistically significant difference was detected in *TNF-α* mRNA levels in either of the groups analyzed. Thus, collectively, our results suggest that L + P therapy had a significant impact on the neocortical glial response, as well as the regulation of inflammation, in APP/PS1 mice, but did not have an effect on hippocampal microgliosis in this model.

4. Discussion

AD is a complex and irreversible neurodegenerative disorder characterized by the slowly progressive loss of cognitive function associated with specific pathologic changes to the brain [1,2]. The underlying pathogenesis of AD is not fully understood, and although there have been numerous therapeutic agents proposed for AD, there have been no effective treatments developed to date. Notably, the main focus of such investigations has been on single-agent therapies. Given the dearth of currently available therapeutic candidates, examining and combining drugs that have been used in human clinical trials for other indications, but with potential to target pathologic and protective mechanisms of relevance to neurodegeneration, may represent a new approach to ameliorating the sequence of cellular changes underlying AD. The present study provides the first experimental evidence for the beneficial actions of L + P combination in the APP/PS1 Tg model of early AD pathology.

Experimental studies have demonstrated the beneficial effect of TZD treatments and leptin therapy on restored cerebrovascular function [20] and improving learning and cognitive decline in AD [8,12,15,20,49,50]. For example, rosiglitazone has been reported to prevent memory deficits induced by Aβ oligomers in Wistar rats [51]. In the J20 AD Tg mouse model, treatment with rosiglitazone reduced memory deficits in object recognition and the Morris water maze (MWM) test [52]. Rosiglitazone also improves spatial memory in APP/PS1 mice [53,54]. In addition, pioglitazone improved reversal learning in adult A/T bi-Tg mice [50]. In 3xTg AD mice, long-term (4 months) pioglitazone treatment improved learning in a hippocampus-dependent task [49] and MWM test [55]. In addition, in APP/PS1 mice, pioglitazone treatment resulted in significant behavioral improvement evaluated by a contextual fear-conditioning assay [56]. Importantly, clinical trials showed significant positive effects of pioglitazone on cognitive outcomes in patients with mild AD [22]. However, the pathways through which these drugs modulate cognitive decline and Aβ-related pathology are not yet completely understood. Indeed, some contradictory

L + P mice ($^{\#}P < .05$ post hoc Sidak's multiple comparison test). A statistically significant reduction of GFAP was observed in WT treated mice relative to WT VH ($^{*}P < .01$). L + P therapy significantly decreased GFAP levels in APP/PS1 mice compared to VH-treated mice ($^{\$}P < .0001$ post hoc Sidak's multiple comparison test). Iba1 expression was significantly higher in APP/PS1 VH mice relative to both WT VH and WT L + P mice ($^{*\,\#}P < .001$ post hoc Sidak's multiple comparison test), while L + P therapy significantly decreased neocortical Iba1 levels in APP/PS1 mice compared to VH-treated mice ($^{\$}P < .0001$ post hoc Sidak's multiple comparison test). In the hippocampus, GFAP expression was significantly higher in APP/PS1 VH mice compared to WT VH ($^{*}P < .0001$) and relative to WT L + P mice ($^{\#}P < .05$ post hoc Sidak's multiple comparison test). L + P therapy significantly decreased GFAP levels in APP/PS1 mice compared with VH-treated mice ($^{\$}P < .01$ post hoc Sidak's multiple comparison test). Iba1 expression was significantly higher in the hippocampus of APP/PS1 VH and APP/PS1 L + P mice groups compared to WT VH controls ($^{*}P < .0001$) and relative to WT L + P ($^{\#}P < .05$ post hoc Sidak's multiple comparison test). L + P therapy did not affect the Iba1 expression levels in APP/PS1 mice compared to VH treated. The data are presented as a percentage (%) of the corresponding value in the WT VH-treated control group. Bar graphs represent the mean ± standard error of the mean. Statistical analyses were performed by two-way analysis of variance followed by Dunnett test, unless stated otherwise. Abbreviation: CTX, neocortex. Scale bars = 20 μm.

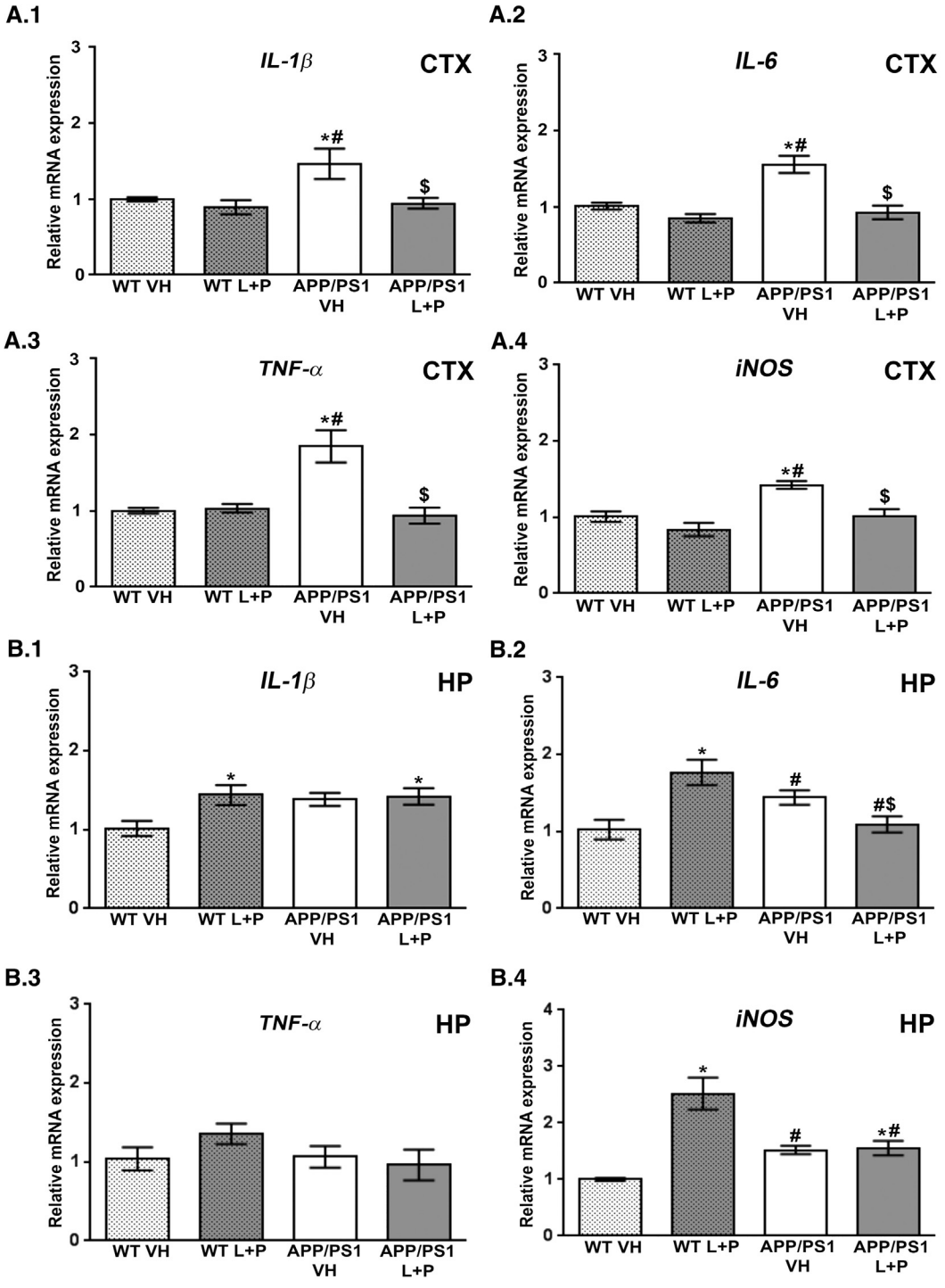

Fig. 5. Leptin and pioglitazone treatment altering the expression of genes involved in inflammation and oxidative stress in the brain. (A.1–4) In the neocortex, RT-qPCR analysis demonstrated a statistically significant upregulation of *IL-1*β, *IL-6*, *TNF-*α, and *iNOS* transcripts in APP/PS1 VH mice relative to WT VH mice (*$P < .01$) and *IL-1*β, *IL-6*, and *iNOS* relative to WT L + P mice ($^{\#}P < .001$ post hoc Sidak's multiple comparison test). L + P therapy significantly downregulated *IL-1*β, *IL-6*, *TNF-*α, and *iNOS* transcripts in APP/PS1 mice compared to VH-treated mice ($^{\$}P < .001$ post hoc Sidak's multiple comparison test). (B.1–4) In the hippocampus, RT-qPCR analysis demonstrated a statistically significant upregulation of *IL-1*β, *IL-6*, and *iNOS* transcripts in WT L + P mice relative to WT VH controls (*$P < .05$ and *$P < .001$), while only *IL-1*β transcript was upregulated in APP/PS1 L + P mice relative to WT VH controls (*$P < .05$). In addition, *IL-6* and *iNOS* transcripts were significantly downregulated in APP/PS1 VH mice compared to WT L + P ($^{\#}P < .0001$, $^{\#}P < .01$ post hoc Sidak's multiple comparison test), while L + P therapy significantly downregulated *IL-6* mRNA in APP/PS1 mice compared to APP/PS1 VH mice ($^{\$}P < .05$ post hoc Sidak's multiple comparison test) and *iNOS* transcript compared to WT L + P ($^{\#}P < .001$ post hoc Sidak's multiple comparison test). No changes in *TNF-*α transcript were found across groups analyzed. The data are presented as a percentage (%) of the corresponding value in the WT VH-treated control group. Bar graphs represent the mean ± standard error of the mean. Statistical analyses were performed by two-way analysis of variance followed by Dunnett test, unless stated otherwise. Abbreviation: CTX, neocortex.

data have been reported. For example, results from Heneka et al. [19] showed that pioglitazone regulates brain Aβ levels through a mechanism involving its capacity to reduce the transcription and expression of β-site amyloid precursor protein cleaving enzyme 1 (BACE1). Other studies demonstrated that the decrease in Aβ levels produced by pioglitazone is related to the Aβ degradation rather than attributable to its transcriptional regulation capacity through the amyloidogenic pathway [56,57]. However, there is a growing consensus that the effect of pioglitazone in decreasing Aβ pathology is mediated by the capacity of this drug to rapidly inhibit inflammatory responses in the brain and negatively modulate amyloidogenesis [58]. In addition, the effect of pioglitazone and other PPARs agonists had variable results in decreasing soluble Aβ species [19,59–62], Aβ plaques [52–54], or both [19,52,56,63]. Conversely, other studies demonstrated no effect on Aβ pathology [20,61,64]. Indeed, in previous studies using APP/PS1 mice, pioglitazone failed to reduce Aβ levels significantly, even when administered for more than 3 months [61]. In contrast, leptin has a strong in vitro [9,13,14] and in vivo [9] amyloidogenic effect, attributable to its transcriptional regulation capacity [10] and inhibition of amyloid precursor protein (APP) processing [12] through the amyloidogenic pathway. It has been demonstrated that leptin improves cognitive function by mechanisms of action closely linked to the regulation of brain Aβ levels. Our findings showed that L + P treatment improved short-term recognition memory loss in APP/PS1 mice and significantly reduced hippocampal fibrillar Aβ burden and brain soluble $A\beta_{1-42}$ levels, while not affecting hippocampal *APP* transcripts. Thus, our preliminary results suggest that combination L + P therapy improves hippocampus-dependent memory and reduces brain Aβ levels, possibly by a mechanism related to Aβ degradation rather than altering processing of APP protein.

Leptin and pioglitazone have been previously shown to reduce tau phosphorylation [52,65–69]. Notably, the APP/PS1 mouse model of AD lacks substantial tau pathology [70] but does demonstrate Aβ plaque–associated DNs with these abnormal axons showing accumulations of neurofilaments, including the triplet proteins (NF-L, NF-M, and NF-H), as well as α-internexin [41,42]. Such plaque-associated DNs may represent one of the earliest forms of neuronal pathology characterizing the preclinical phase of AD [71]. NF triplet containing pyramidal neurons, providing corticocortical connectivity, is also selectively vulnerable to AD pathology [72–76], and NF-L gene deletion is associated with increased Aβ deposition in the APP/PS1 model [41]. In addition, NF-containing DNs are the earliest neuronal change associated with Aβ plaque formation in the human brain [45,46]. In the present study, L + P treatment significantly decreased neocortical NF-containing DNs, which may be indicative of reduced damage to corticocortical circuitry [77].

Because Aβ induces synaptic loss in AD, we evaluated expression levels of synaptic proteins as these are important molecular markers of AD-affected brain regions. Synapse loss has been reported to occur very early in AD [78,79] and has been shown to correlate well with cognitive decline [78–80]. Using immunohistochemistry analysis, we have previously demonstrated the specific vulnerability of excitatory synapses in close proximity to Aβ plaques in 9- and 12-month-old APP/PS1 mice [41,81]. In agreement with previous data [82], immunoblotting revealed no changes in SYN expression in both neocortex/hippocampus homogenates in APP/PS1 mice compared with WT controls. In addition, our study confirms our reported data [81], demonstrating that vGLUT1 and GAD65/67 expression was unchanged in APP/PS1 mice compared with WT mice. We also observed an increase in hippocampal GAD65/67 expression in WT treated mice compared with WT VH controls, a result that was unexpected but which may highlight the involvement of leptin in synaptic plasticity [83]. Accordingly, leptin activates a postsynaptic molecular signaling pathway to potentiate developing GABAergic synapses in the hippocampus [84]. Indeed, obese diabetic mice lacking leptin receptor (db/db) have a reduced density in dendritic spines and an immature pattern of synaptic proteins [85–88]. Interestingly, L + P treatment significantly increased hippocampal PSD-95 levels in APP/PS1 mice, perhaps reflecting the effectiveness of combination therapy on reducing postsynaptic damage, potentially by compensatory mechanisms, that correlates with the behavioral deficit observed in APP/PS1 mice. Indeed, PSD-95, the most abundant scaffolding protein in the excitatory postsynaptic density [23], has been shown to decline in association with progression of memory deficits in AD [89,90].

Inflammation and the immune response have been proposed to contribute to the pathogenesis of AD. Reactive glial cells associated with Aβ plaques and its inflammatory components may contribute to the synapse loss and dysfunction in AD [91]. Furthermore, we were particularly interested in the effect of L + P treatment on the inflammatory response associated with AD, as the role of pioglitazone in inflammation in AD has been extensively investigated previously. For example, the capacity of this agent to rapidly inhibit inflammatory responses in the brain has been demonstrated in several murine models of AD [19,20]. Conversely, the role of leptin in inflammation in AD is poorly understood. Leptin has been associated with inflammation and immune responses [92], and an active interaction of the central nervous system with the immune system through cytokines and other inflammatory factors has been described [93]. The present study confirms reports [94] demonstrating a significant increase in GFAP and Iba1 expression in both neocortex and hippocampus of APP/PS1 mice relative to WT controls, which corresponded with

a general upregulation of *IL-1β, IL-6, TNF-α,* and *iNOS* transcripts. However, L + P treatment was associated with significantly reduced neocortical expression of GFAP and Iba1 proteins in APP/PS1 mice, concomitant with the downregulation of *IL-1β, IL-6, TNF-α*, and *iNOS* transcripts to the basal mRNA levels detected in WT control mice. In the hippocampus, the treatment was associated with reduced expression of the astroglial response, corresponding with a significant downregulation of *iNOS* transcript [19], while reactive microglia were relatively unaffected, perhaps reflecting differences in the effectiveness of L + P treatment in the two brain regions tested.

Another unexpected finding of this project was increased hippocampal Iba1 protein concomitant with the upregulation of *IL-1β, IL-6,* and *iNOS* transcripts in WT L + P treated mice, which may support the involvement of leptin in neuroinflammation. Previous reports have shown that this hormone modulates the activation of both peripheral immune cells and brain microglia [95,96]. Furthermore, in the aging brain, there is a decline in the normal antioxidant defense mechanisms [97] as well as a vascular disease progress [98]. Reflecting an inflammatory component, *iNOS* is expressed in macrophages and glial cells in response to proinflammatory cytokines under pathologic conditions such as AD, in which there is increased permeability of the blood-brain barrier (BBB). However, it has also recently been determined that *iNOS* can also serve as a negative feedback regulator, preventing the influx of inflammatory cells by restoring the integrity of the BBB [99]. Our data indicated that combination L + P therapy significantly upregulated *iNOS* expression in WT treated mice, which may confer a defense against the normal changes in the vasculature preventing the influx of inflammatory cells to the brain. Future studies will be necessary to further explain these unexpected results; however, they may highlight the involvement of leptin in immune responses and inflammation within the brain.

In summary, the data reported here provide the first preliminary experimental evidence for the beneficial effect of combining leptin and pioglitazone drugs in treating AD. Our data support the potential effectiveness of combinatorial therapies for the possible inhibition of AD-related pathologic brain changes. However, as both leptin and pioglitazone compounds were not tested independently under the same experimental conditions, future studies will be necessary to further determine whether combining L + P treatment might be more beneficial than using both drugs independently on improving learning and the regulation of brain Aβ levels in AD.

Acknowledgments

The authors would like to gratefully acknowledge Graeme McCormack and Justin Dittmann for their excellent technical support. The authors declare that they have no conflict of interest. This work was supported by the funding from J.O. and J.R. Wicking Trust (Equity Trustees).

Supplementary data

Supplementary data related to this article can be found at http://dx.doi.org/10.1016/j.trci.2016.11.002.

RESEARCH IN CONTEXT

1. Systematic review: The lack of effective treatment for Alzheimer's disease (AD) has promoted a call for the development of combination therapies to tackle the multifactorial nature of AD. The drugs leptin and pioglitazone have shown substantial promise as monotherapies in AD. However, no studies have investigated the effects of these therapeutic agents in combination for AD.
2. Interpretation: We studied the impact of acute combined leptin and pioglitazone treatment on the transgenic APP/PS1 mouse model of AD. Our results support that the neuroprotective effect of leptin in combination with the anti-inflammatory action of pioglitazone significantly reduces the pathologic features that characterize AD.
3. Future directions: Our data provided evidence for synergistic actions of leptin and pioglitazone, which may suggest a novel and improved therapeutic approach for treatment of this devastating disease. Future studies will be necessary to further support the use of this combination therapy in the treatment of AD.

References

[1] Hyman BT, Damasio H, Damasio AR, Van Hoesen GW. Alzheimer's disease. Annu Rev Public Health 1989;10:115–40.
[2] Villemagne VL, Burnham S, Bourgeat P, Brown B, Ellis KA, Salvado O, et al. Amyloid beta deposition, neurodegeneration, and cognitive decline in sporadic Alzheimer's disease: a prospective cohort study. Lancet Neurol 2013;12:357–67.
[3] Chow VW, Savonenko AV, Melnikova T, Kim H, Price DL, Li T, et al. Modeling an anti-amyloid combination therapy for Alzheimer's disease. Sci Transl Med 2010;2:13ra1.
[4] Jacobsen H, Ozmen L, Caruso A, Narquizian R, Hilpert H, Jacobsen B, et al. Combined treatment with a BACE inhibitor and anti-Abeta antibody gantenerumab enhances amyloid reduction in APPLondon mice. J Neurosci 2014;34:11621–30.
[5] Skerrett R, Pellegrino MP, Casali BT, Taraboanta L, Landreth GE. Combined Liver X Receptor/Peroxisome Proliferator-activated Receptor gamma Agonist Treatment Reduces Amyloid beta Levels and Improves Behavior in Amyloid Precursor Protein/Presenilin 1 Mice. J Biol Chem 2015;290:21591–602.

[6] Stephens TW, Basinski M, Bristow PK, Bue-Valleskey JM, Burgett SG, Craft L, et al. The role of neuropeptide Y in the antiobesity action of the obese gene product. Nature 1995;377:530–2.
[7] Zhang Y, Proenca R, Maffei M, Barone M, Leopold L, Friedman JM. Positional cloning of the mouse obese gene and its human homologue. Nature 1994;372:425–32.
[8] Greco SJ, Bryan KJ, Sarkar S, Zhu X, Smith MA, Ashford JW, et al. Leptin reduces pathology and improves memory in a transgenic mouse model of Alzheimer's disease. J Alzheimers Dis 2010;19:1155–67.
[9] Fewlass DC, Noboa K, Pi-Sunyer FX, Johnston JM, Yan SD, Tezapsidis N. Obesity-related leptin regulates Alzheimer's Abeta. FASEB J 2004;18:1870–8.
[10] Niedowicz DM, Studzinski CM, Weidner AM, Platt TL, Kingry KN, Beckett TL, et al. Leptin regulates amyloid beta production via the gamma-secretase complex. Biochim Biophys Acta 2013;1832:439–44.
[11] Marwarha G, Dasari B, Prasanthi JR, Schommer J, Ghribi O. Leptin reduces the accumulation of Abeta and phosphorylated tau induced by 27-hydroxycholesterol in rabbit organotypic slices. J Alzheimers Dis 2014;19:1007–19.
[12] Perez-Gonzalez R, Alvira-Botero MX, Robayo O, Antequera D, Garzon M, Martin-Moreno AM, et al. Leptin gene therapy attenuates neuronal damages evoked by amyloid-beta and rescues memory deficits in APP/PS1 mice. Gene Ther 2014;21:298–308.
[13] Greco SJ, Sarkar S, Johnston JM, Zhu X, Su B, Casadesus G, et al. Leptin reduces Alzheimer's disease-related tau phosphorylation in neuronal cells. Biochem Biophys Res Commun 2008;376:536–41.
[14] Greco SJ, Sarkar S, Johnston JM, Tezapsidis N. Leptin regulates tau phosphorylation and amyloid through AMPK in neuronal cells. Biochem Biophys Res Commun 2009;380:98–104.
[15] Farr SA, Banks WA, Morley JE. Effects of leptin on memory processing. Peptides 2006;27:1420–5.
[16] Moult PR, Milojkovic B, Harvey J. Leptin reverses long-term potentiation at hippocampal CA1 synapses. J Neurochem 2009;108:685–96.
[17] Harvey J. Leptin: a diverse regulator of neuronal function. J Neurochem 2007;100:307–13.
[18] Feinstein DL. Therapeutic potential of peroxisome proliferator-activated receptor agonists for neurological disease. Diabetes Technol Ther 2003;5:67–73.
[19] Heneka MT, Sastre M, Dumitrescu-Ozimek L, Hanke A, Dewachter I, Kuiperi C, et al. Acute treatment with the PPARgamma agonist pioglitazone and ibuprofen reduces glial inflammation and Abeta1-42 levels in APPV717I transgenic mice. Brain 2005;128:1442–53.
[20] Nicolakakis N, Aboulkassim T, Ongali B, Lecrux C, Fernandes P, Rosa-Neto P, et al. Complete rescue of cerebrovascular function in aged Alzheimer's disease transgenic mice by antioxidants and pioglitazone, a peroxisome proliferator-activated receptor gamma agonist. J Neurosci 2008;28:9287–96.
[21] Esposito K, Ciotola M, Merante D, Giugliano D. Rosiglitazone cools down inflammation in the metabolic syndrome. Arterioscler Thromb Vasc Biol 2006;26:1413–4.
[22] Sato T, Hanyu H, Hirao K, Kanetaka H, Sakurai H, Iwamoto T. Efficacy of PPAR-gamma agonist pioglitazone in mild Alzheimer disease. Neurobiol Aging 2011;32:1626–33.
[23] Wang TD, Chen WJ, Cheng WC, Lin JW, Chen MF, Lee YT. Relation of improvement in endothelium-dependent flow-mediated vasodilation after rosiglitazone to changes in asymmetric dimethylarginine, endothelin-1, and C-reactive protein in nondiabetic patients with the metabolic syndrome. Am J Cardiol 2006;98:1057–62.
[24] Fernandez-Martos CM, Gonzalez P, Rodriguez FJ. Acute leptin treatment enhances functional recovery after spinal cord injury. PLoS One 2012;7:e35594.
[25] Garcia-Alloza M, Robbins EM, Zhang-Nunes SX, Purcell SM, Betensky RA, Raju S, et al. Characterization of amyloid deposition in the APPswe/PS1dE9 mouse model of Alzheimer disease. Neurobiol Dis 2006;24:516–24.
[26] Kamphuis W, Mamber C, Moeton M, Kooijman L, Sluijs JA, Jansen AH, et al. GFAP isoforms in adult mouse brain with a focus on neurogenic astrocytes and reactive astrogliosis in mouse models of Alzheimer disease. PLoS One 2012;7:e42823.
[27] Jankowsky JL, Fadale DJ, Anderson J, Xu GM, Gonzales V, Jenkins NA, et al. Mutant presenilins specifically elevate the levels of the 42 residue beta-amyloid peptide in vivo: evidence for augmentation of a 42-specific gamma secretase. Hum Mol Genet 2004;13:159–70.
[28] Fliedner S, Schulz C, Lehnert H. Brain uptake of intranasally applied radioiodinated leptin in Wistar rats. Endocrinology 2006;147:2088–94.
[29] Collino M, Aragno M, Mastrocola R, Gallicchio M, Rosa AC, Dianzani C, et al. Modulation of the oxidative stress and inflammatory response by PPAR-gamma agonists in the hippocampus of rats exposed to cerebral ischemia/reperfusion. Eur J Pharmacol 2006;530:70–80.
[30] Arnold JJ, Ahsan F, Meezan E, Pillion DJ. Correlation of tetradecylmaltoside induced increases in nasal peptide drug delivery with morphological changes in nasal epithelial cells. J Pharm Sci 2004;93:2205–13.
[31] Chuah MI, Tennent R, Jacobs I. Response of olfactory Schwann cells to intranasal zinc sulfate irrigation. J Neurosci Res 1995;42:470–8.
[32] Harris JA, West AK, Chuah MI. Olfactory ensheathing cells: nitric oxide production and innate immunity. Glia 2009;57:1848–57.
[33] Adeosun SO, Hou X, Zheng B, Stockmeier C, Ou X, Paul I, et al. Cognitive deficits and disruption of neurogenesis in a mouse model of apolipoprotein E4 domain interaction. J Biol Chem 2014;289:2946–59.
[34] Liu Y, Staal JA, Canty AJ, Kirkcaldie MT, King AE, Bibari O, et al. Cytoskeletal changes during development and aging in the cortex of neurofilament light protein knockout mice. J Comp Neurol 2013;521:1817–27.
[35] Fernandez CM, Molto E, Gallardo N, del Arco A, Martinez C, Andres A, et al. The expression of rat resistin isoforms is differentially regulated in visceral adipose tissues: effects of aging and food restriction. Metabolism 2009;58:204–11.
[36] Petrov D, Pedros I, Artiach G, Sureda FX, Barroso E, Pallas M, et al. High-fat diet-induced deregulation of hippocampal insulin signaling and mitochondrial homeostasis deficiences contribute to Alzheimer disease pathology in rodents. Biochim Biophys Acta 2015;1852:1687–99.
[37] Fernandez-Martos CM, Gonzalez-Fernandez C, Gonzalez P, Maqueda A, Arenas E, Rodriguez FJ. Differential expression of Wnts after spinal cord contusion injury in adult rats. PLoS One 2011;6:e27000.
[38] Livak KJ, Schmittgen TD. Analysis of relative gene expression data using real-time quantitative PCR and the 2(-Delta Delta C(T)) Method. Methods 2001;25:402–8.
[39] Gonzalez-Fernandez C, Fernandez-Martos CM, Shields SD, Arenas E, Javier Rodriguez F. Wnts are expressed in the spinal cord of adult mice and are differentially induced after injury. J Neurotrauma 2014;31:565–81.
[40] Liu Y, Atkinson RA, Fernandez-Martos CM, Kirkcaldie MT, Cui H, Vickers JC, et al. Changes in TDP-43 expression in development, aging, and in the neurofilament light protein knockout mouse. Neurobiol Aging 2015;36:1151–9.
[41] Fernandez-Martos CM, King AE, Atkinson RA, Woodhouse A, Vickers JC. Neurofilament light gene deletion exacerbates amyloid, dystrophic neurite, and synaptic pathology in the APP/PS1 transgenic model of Alzheimer's disease. Neurobiol Aging 2015;36:2757–67.
[42] Mitew S, Kirkcaldie MT, Dickson TC, Vickers JC. Neurites containing the neurofilament-triplet proteins are selectively vulnerable to cytoskeletal pathology in Alzheimer's disease and transgenic mouse models. Front Neuroanat 2013;7:30.
[43] Collins JM, King AE, Woodhouse A, Kirkcaldie MT, Vickers JC. The effect of focal brain injury on beta-amyloid plaque deposition, inflammation and synapses in the APP/PS1 mouse model of Alzheimer's disease. Exp Neurol 2015;267:219–29.
[44] Franklin KBJ, Paxinos G. The Mouse Brain in Stereotaxic Coordinates. New York, NY: Academic Press; 2008.

[45] Dickson TC, King CE, McCormack GH, Vickers JC. Neurochemical diversity of dystrophic neurites in the early and late stages of Alzheimer's disease. Exp Neurol 1999;156:100–10.
[46] Vickers JC, Chin D, Edwards AM, Sampson V, Harper C, Morrison J. Dystrophic neurite formation associated with age-related beta amyloid deposition in the neocortex: clues to the genesis of neurofibrillary pathology. Exp Neurol 1996;141:1–11.
[47] Le R, Cruz L, Urbanc B, Knowles RB, Hsiao-Ashe K, Duff K, et al. Plaque-induced abnormalities in neurite geometry in transgenic models of Alzheimer disease: implications for neural system disruption. J Neuropathol Exp Neurol 2001;60:753–8.
[48] Woodhouse A, Vickers JC, Adlard PA, Dickson TC. Dystrophic neurites in TgCRND8 and Tg2576 mice mimic human pathological brain aging. Neurobiol Aging 2009;30:864–74.
[49] Searcy JL, Phelps JT, Pancani T, Kadish I, Popovic J, Anderson KL, et al. Long-term pioglitazone treatment improves learning and attenuates pathological markers in a mouse model of Alzheimer's disease. J Alzheimers Dis 2012;30:943–61.
[50] Papadopoulos P, Rosa-Neto P, Rochford J, Hamel E. Pioglitazone improves reversal learning and exerts mixed cerebrovascular effects in a mouse model of Alzheimer's disease with combined amyloid-beta and cerebrovascular pathology. PLoS One 2013;8:e68612.
[51] Xu S, Guan Q, Wang C, Wei X, Chen X, Zheng B, et al. Rosiglitazone prevents the memory deficits induced by amyloid-beta oligomers via inhibition of inflammatory responses. Neurosci Lett 2014;578:7–11.
[52] Escribano L, Simon AM, Gimeno E, Cuadrado-Tejedor M, Lopez de Maturana R, Garcia-Osta A, et al. Rosiglitazone rescues memory impairment in Alzheimer's transgenic mice: mechanisms involving a reduced amyloid and tau pathology. Neuropsychopharmacology 2010;35:1593–604.
[53] O'Reilly JA, Lynch M. Rosiglitazone improves spatial memory and decreases insoluble Abeta(1-42) in APP/PS1 mice. J Neuroimmune Pharmacol 2012;7:140–4.
[54] Toledo EM, Inestrosa NC. Activation of Wnt signaling by lithium and rosiglitazone reduced spatial memory impairment and neurodegeneration in brains of an APPswe/PSEN1DeltaE9 mouse model of Alzheimer's disease. Mol Psychiatry 2010;15:272–85. 228.
[55] Yu Y, Li X, Blanchard J, Li Y, Iqbal K, Liu F, et al. Insulin sensitizers improve learning and attenuate tau hyperphosphorylation and neuroinflammation in 3xTg-AD mice. J Neural Transm (Vienna) 2015; 122:593–606.
[56] Mandrekar-Colucci S, Karlo JC, Landreth GE. Mechanisms underlying the rapid peroxisome proliferator-activated receptor-gamma-mediated amyloid clearance and reversal of cognitive deficits in a murine model of Alzheimer's disease. J Neurosci 2012;32:10117–28.
[57] Camacho IE, Serneels L, Spittaels K, Merchiers P, Dominguez D, De Strooper B. Peroxisome-proliferator-activated receptor gamma induces a clearance mechanism for the amyloid-beta peptide. J Neurosci 2004;24:10908–17.
[58] Perez MJ, Quintanilla RA. Therapeutic Actions of the Thiazolidinediones in Alzheimer's Disease. PPAR Res 2015;2015:957248.
[59] Lacombe P, Mathews PM, Schmidt SD, Breidert T, Heneka MT, Landreth GE, et al. Effect of anti-inflammatory agents on transforming growth factor beta over-expressing mouse brains: a model revised. J Neuroinflammation 2004;1:11.
[60] Pedersen WA, McMillan PJ, Kulstad JJ, Leverenz JB, Craft S, Haynatzki GR. Rosiglitazone attenuates learning and memory deficits in Tg2576 Alzheimer mice. Exp Neurol 2006;199:265–73.
[61] Yan Q, Zhang J, Liu H, Babu-Khan S, Vassar R, Biere AL, et al. Anti-inflammatory drug therapy alters beta-amyloid processing and deposition in an animal model of Alzheimer's disease. J Neurosci 2003; 23:7504–9.
[62] Amantea D, Tassorelli C, Russo R, Petrelli F, Morrone LA, Bagetta G, et al. Neuroprotection by leptin in a rat model of permanent cerebral ischemia: effects on STAT3 phosphorylation in discrete cells of the brain. Cell Death Dis 2011;2:e238.
[63] Yamanaka M, Ishikawa T, Griep A, Axt D, Kummer MP, Heneka MT. PPARgamma/RXRalpha-induced and CD36-mediated microglial amyloid-beta phagocytosis results in cognitive improvement in amyloid precursor protein/presenilin 1 mice. J Neurosci 2012;32:17321–31.
[64] Denner LA, Rodriguez-Rivera J, Haidacher SJ, Jahrling JB, Carmical JR, Hernandez CM, et al. Cognitive enhancement with rosiglitazone links the hippocampal PPARgamma and ERK MAPK signaling pathways. J Neurosci 2012;32:16725a–35.
[65] Escribano L, Simon AM, Perez-Mediavilla A, Salazar-Colocho P, Del Rio J, Frechilla D. Rosiglitazone reverses memory decline and hippocampal glucocorticoid receptor down-regulation in an Alzheimer's disease mouse model. Biochem Biophys Res Commun 2009; 379:406–10.
[66] To AW, Ribe EM, Chuang TT, Schroeder JE, Lovestone S. The epsilon3 and epsilon4 alleles of human APOE differentially affect tau phosphorylation in hyperinsulinemic and pioglitazone treated mice. PLoS One 2011;6:e16991.
[67] Liu F, Li B, Tung EJ, Grundke-Iqbal I, Iqbal K, Gong CX. Site-specific effects of tau phosphorylation on its microtubule assembly activity and self-aggregation. Eur J Neurosci 2007;26:3429–36.
[68] Lovestone S, Davis DR, Webster MT, Kaech S, Brion JP, Matus A, et al. Lithium reduces tau phosphorylation: effects in living cells and in neurons at therapeutic concentrations. Biol Psychiatry 1999; 45:995–1003.
[69] Greco SJ, Sarkar S, Casadesus G, Zhu X, Smith MA, Ashford JW, et al. Leptin inhibits glycogen synthase kinase-3beta to prevent tau phosphorylation in neuronal cells. Neurosci Lett 2009;455:191–4.
[70] Howlett DR, Bowler K, Soden PE, Riddell D, Davis JB, Richardson JC, et al. Abeta deposition and related pathology in an APP x PS1 transgenic mouse model of Alzheimer's disease. Histol Histopathol 2008;23:67–76.
[71] Vickers JC, Mitew S, Woodhouse A, Fernandez-Martos CM, Kirkcaldie MT, Canty AJ, et al. Defining the earliest pathological changes of Alzheimer's disease. Curr Alzheimer Res 2016;13:281–7.
[72] Hof PR, Morrison JH. Neocortical neuronal subpopulations labeled by a monoclonal antibody to calbindin exhibit differential vulnerability in Alzheimer's disease. Exp Neurol 1991;111:293–301.
[73] Morrison JH, Lewis DA, Campbell MJ, Huntley GW, Benson DL, Bouras C. A monoclonal antibody to non-phosphorylated neurofilament protein marks the vulnerable cortical neurons in Alzheimer's disease. Brain Res 1987;416:331–6.
[74] Vickers JC, Costa M. The neurofilament triplet is present in distinct subpopulations of neurons in the central nervous system of the guinea-pig. Neuroscience 1992;49:73–100.
[75] Vickers JC, Riederer BM, Marugg RA, Buee-Scherrer V, Buee L, Delacourte A, et al. Alterations in neurofilament protein immunoreactivity in human hippocampal neurons related to normal aging and Alzheimer's disease. Neuroscience 1994;62:1–13.
[76] Vickers JC, Delacourte A, Morrison JH. Progressive transformation of the cytoskeleton associated with normal aging and Alzheimer's disease. Brain Res 1992;594:273–8.
[77] Duyckaerts C, Sazdovitch V, Seilhean D, Delaere P, Hauw JJ. A brain bank in a neuropathology laboratory (with some emphasis on diagnostic criteria). J Neural Transm Suppl 1993;39:107–18.
[78] Scheff SW, Price DA, Schmitt FA, Mufson EJ. Hippocampal synaptic loss in early Alzheimer's disease and mild cognitive impairment. Neurobiol Aging 2006;27:1372–84.
[79] Terry RD, Masliah E, Salmon DP, Butters N, DeTeresa R, Hill R, et al. Physical basis of cognitive alterations in Alzheimer's disease: synapse loss is the major correlate of cognitive impairment. Ann Neurol 1991; 30:572–80.
[80] Knafo S, Alonso-Nanclares L, Gonzalez-Soriano J, Merino-Serrais P, Fernaud-Espinosa I, Ferrer I, et al. Widespread changes in dendritic spines in a model of Alzheimer's disease. Cereb Cortex 2009;19:586–92.
[81] Mitew S, Kirkcaldie MT, Dickson TC, Vickers JC. Altered synapses and gliotransmission in Alzheimer's disease and AD model mice. Neurobiol Aging 2013;34:2341–51.

[82] Pedros I, Petrov D, Allgaier M, Sureda F, Barroso E, Beas-Zarate C, et al. Early alterations in energy metabolism in the hippocampus of APPswe/PS1dE9 mouse model of Alzheimer's disease. Biochim Biophys Acta 2014;1842:1556–66.
[83] Harvey J, Solovyova N, Irving A. Leptin and its role in hippocampal synaptic plasticity. Prog Lipid Res 2006;45:369–78.
[84] Guimond D, Diabira D, Porcher C, Bader F, Ferrand N, Zhu M, et al. Leptin potentiates GABAergic synaptic transmission in the developing rodent hippocampus. Front Cell Neurosci 2014;8:235.
[85] Ahima RS, Bjorbaek C, Osei S, Flier JS. Regulation of neuronal and glial proteins by leptin: implications for brain development. Endocrinology 1999;140:2755–62.
[86] Stranahan AM, Lee K, Martin B, Maudsley S, Golden E, Cutler RG, et al. Voluntary exercise and caloric restriction enhance hippocampal dendritic spine density and BDNF levels in diabetic mice. Hippocampus 2009;19:951–61.
[87] Udagawa J, Hashimoto R, Suzuki H, Hatta T, Sotomaru Y, Hioki K, et al. The role of leptin in the development of the cerebral cortex in mouse embryos. Endocrinology 2006;147:647–58.
[88] Udagawa J, Hatta T, Hashimoto R, Otani H. Roles of leptin in prenatal and perinatal brain development. Congenit Anom (Kyoto) 2007; 47:77–83.
[89] Oakley H, Cole SL, Logan S, Maus E, Shao P, Craft J, et al. Intraneuronal beta-amyloid aggregates, neurodegeneration, and neuron loss in transgenic mice with five familial Alzheimer's disease mutations: potential factors in amyloid plaque formation. J Neurosci 2006; 26:10129–40.
[90] Shao CY, Mirra SS, Sait HB, Sacktor TC, Sigurdsson EM. Postsynaptic degeneration as revealed by PSD-95 reduction occurs after advanced Abeta and tau pathology in transgenic mouse models of Alzheimer's disease. Acta Neuropathol 2011;122:285–92.
[91] Zhang F, Jiang L. Neuroinflammation in Alzheimer's disease. Neuropsychiatr Dis Treat 2015;11:243–56.
[92] Munshi S. Clinicotherapeutic Potential of Leptin in Alzheimer's Disease and Parkinson's Disease. Asian J Neurosci 2014;2014:9.
[93] Carson MJ, Doose JM, Melchior B, Schmid CD, Ploix CC. CNS immune privilege: hiding in plain sight. Immunol Rev 2006;213:48–65.
[94] Jaffar S, Counts SE, Ma SY, Dadko E, Gordon MN, Morgan D, et al. Neuropathology of mice carrying mutant APP(swe) and/or PS1(M146L) transgenes: alterations in the p75(NTR) cholinergic basal forebrain septohippocampal pathway. Exp Neurol 2001;170:227–43.
[95] Aguilar-Valles A, Inoue W, Rummel C, Luheshi GN. Obesity, adipokines and neuroinflammation. Neuropharmacology 2015;96:124–34.
[96] Lafrance V, Inoue W, Kan B, Luheshi GN. Leptin modulates cell morphology and cytokine release in microglia. Brain Behav Immun 2010;24:358–65.
[97] Finkel T, Holbrook NJ. Oxidants, oxidative stress and the biology of ageing. Nature 2000;408:239–47.
[98] Rosenberg GA. Blood-Brain Barrier Permeability in Aging and Alzheimer's Disease. J Prev Alzheimers Dis 2014;1:138–9.
[99] Olivera GC, Ren X, Vodnala SK, Lu J, Coppo L, Leepiyasakulchai C, et al. Nitric Oxide Protects against Infection-Induced Neuroinflammation by Preserving the Stability of the Blood-Brain Barrier. Plos Pathog 2016;12:e1005442.